Hydrogen Bronze Formation within Pd/MoO_3 Composites

H. Noh, D. Wang, S. Luo, and Ted B. Flanagan*

Material Science Program and Department of Chemistry, University of Vermont, Burlington, Vermont 05405

R. Balasubramaniam

Department of Materials and Metallurgical Engineering, Indian Institute of Technology, Kanpur 208 016, India

Y. Sakamoto

Department of Materials Science and Engineering, Nagasaki University, 852-8521 Nagasaki, Japan

Received: June 13, 2003; In Final Form: October 21, 2003

In this study, *Pd*−Mo alloys have been internally oxidized to form Pd/MoO_3 composites, and it is shown for the first time that H_2 reacts with these composites to form H-bronzes, for example, H_xMoO_3, within the Pd matrix. The Pd matrix is the source of mobile H atoms, which react with the oxide precipitates to form H-bronzes. The kinetics of H-bronze formation are extremely fast. Solubilities of H_2 in the Pd/MoO_3 composites have been measured, and because H_2 solution in the oxide is so much more exothermic than that in the Pd matrix, the former can be separated from the latter. The intercept of the solubility plot along the H content axis gives the stoichiometry of the H-bronze formed. Some irreproducibility was found in the p_{H_2} versus r relationships, which is also found in H-bronzes prepared by other techniques such as H spillover. The relative partial enthalpies of H_2 solution, ΔH_H, in the H-bronzes have been determined by reaction calorimetry as a function of the H content of the bronze. The ΔH_H values decrease sharply in exothermicity with increasing x in H_xMoO_3.

Introduction

Substitutional fcc *Pd*−Al alloys can be internally oxidized producing Al_2O_3 precipitates within the metal phase.[1] Kirchheim and Huang et al.[2−4] studied the interaction of dissolved hydrogen with Pd containing alumina precipitates prepared by internal oxidation. The dissolved H segregated to the metal/oxide interfaces serving as a probe for the interface properties. Their research concentrated on the low hydrogen content region where hydrogen is trapped both irreversibly and reversibly. The irreversibly held hydrogen was suggested to be bonded to oxygen atoms at the interface forming an interfacial monolayer, which could be removed by evacuation at $T \geq 573$ K. The reversibly held hydrogen could be removed by evacuation at about 423 K and was assumed to originate from a combination of segregation to the stress fields of the precipitates and interaction with chemical species at the interface.[3] Their measurements were carried out electrochemically at 295 K; the hydrogen chemical potential was monitored from the electrode potentials using the Pd/Al_2O_3 composite as one electrode. The upper limit of the hydrogen contents in their study was about $(H/Pd) = r \approx 0.01$.[4] Hydrogen solubilities in internally oxidized *Pd*−Mg, *Pd*−Zr, and *Pd*−Zn alloys were also investigated by these authors.

Noh et al[5] have recently shown that the initial H_2 isotherm after internal oxidation of a $Pd_{0.97}Al_{0.03}$ alloy corresponds to pure Pd aside from the very dilute trapping region. It should be recalled that a Pd−H isotherm has a region at low H contents where H_2 dissolves in the dilute phase of Pd. At a certain H concentration a hydride phase appears. and when this and the dilute phase coexist, the equilibrium p_{H_2} must be constant, the plateau pressure, according to the phase rule. When the hydride phase is fully formed, further H_2 dissolves in it, and p_{H_2} increases markedly with H content.[6]

After repeated cycling, hydriding/dehydriding, of the internally oxidized $Pd_{0.97}Al_{0.03}$ alloy, especially at elevated temperatures, the isotherms differ from Pd−H and have only a small hysteresis.[7] It was also shown that after partial internal oxidation there were two plateau regions, one corresponding to Pd and the other to the unoxidized $Pd_{0.97}Al_{0.03}$ alloy. Hydrogen isotherms can therefore be used to determine the fraction of internal oxidation that occurs.

In the present study, a different type of solute in Pd, that is, Mo, will be internally oxidized and subsequently exposed to H_2, which will be employed as a probe for the characterization of the oxide precipitates. A gas-phase technique will be employed to determine the relative hydrogen chemical potentials, $\mu_H - {}^1/_2\mu^0_{H_2} = \Delta\mu_H = {}^1/_2RT \ln p_{H_2}$ as a function of $(H/M) = r$. Hydrogen solubilities before and after oxidation will be measured over the range from about $r = 0$ to the maximum hydrogen solubilities corresponding to $p_{H_2} \approx 0.5$ MPa.

MoO_3 is known to form a so-called hydrogen bronze, H_xMoO_3.[8−11] A common method used for their preparation is "hydrogen spillover" whereby particles of noble metal such as Pt or Pd are in intimate contact with the oxides. These noble metal particles are sites for the needed H_2 dissociation because the oxides will not absorb hydrogen directly via H_2.[11] The oxide then receives H by diffusion from the metal. H atoms are reported to diffuse rather fast within H_xMoO_3.[12,13] They have been shown to bond within the oxide to O to form OH bonds or to form OH_2 bonds at higher H contents.[14] It has been argued, however, that the H may be delocalized such that these OH or OH_2 bonds may have only a short lifetime.[15]

* Corresponding author. E-mail: flanagan@emba.uvm.edu.

10.1021/jp0307506 CCC: $27.50
Published on Web 12/09/2003

Birtill and Dickens[8] have employed X-ray diffraction analysis (XRD) to identify four different H-bronzes, H_xMO_3, and in each, the basic layer structure of MoO_3 is maintained without a very large lattice expansion due to the H. They also indicated that the various H_xMO_3 compounds are not line compounds, but each has a spread of x values. Susic and Solonin[16] found that heating the H-bronze to 510 K leads to some decomposition of the structure and further heating to 613 K leads to the formation of amorphous H_xMO_3.

In this research, it will be determined whether a H-bronze forms from the Pd/Mo oxide composite prepared by internal oxidation. The main requirement of supplying mobile H atoms will be met by the Pd composite, but it is not known whether the H-bronze will form *within* the Pd matrix.

In addition to gas-phase measurements of p_{H_2} as a function of H/M $= r$ isotherms, calorimetric measurements of the enthalpy changes upon adding or removing small increments of hydrogen will be carried out. Provided that the H-bronzes form, this method for obtaining enthalpies should be valid as argued by Tinet et al[15] despite any irreversibility, which has been reported for these systems.[17] Meaningful enthalpies cannot be obtained from plots of $\Delta\mu_H/T = R \ln p_{H_2}{}^{1/2}$ against $1/T$ at constant r because such data require that equilibrium be attained.

Experimental Section

Substitutional alloys were prepared by arc-melting the pure elements under argon. The buttons were flipped and remelted several times. They were then annealed in vacuo for 72 h at 1133 K, rolled into foils of ~100 μm, and reannealed for 48 h (1133 K). The alloys were then oxidized in air at several different temperatures from 983 to 1273 K for various lengths of time and then quenched into water (273 K) after oxidation. The alloys generally remained ductile after oxidation but became brittle after hydriding/dehydriding.

Relative partial molar enthalpies, $\Delta H_H = H_H - {}^1/_2H^0_{H_2}$, can be obtained from measurements of δq when δn_H mol of ${}^1/_2H_2$ are added to or removed from the alloy at nearly constant H/M $= r$ under psuedo-isothermal conditions, that is,

$$\Delta H_H = (\partial \Delta H/\partial n_H)_{r,T} \approx (\delta q/\delta n_H)_{r,T} \qquad (1)$$

and δq is measured in a dual-cell, heat-leak calorimeter as described elsewhere.[18] In these studies, the composites are essentially "titrated" with H_2, while the heats of reaction are determined for each dose of H_2.

Results and Discussion

Before the results are presented, it should be pointed out that some of the data were anomalous reflecting the inherent irreversibility of H-bronze systems. In some runs when H_2 was "titrated" with the metal/oxide composite, the p_{H_2} was essentially zero during H-bronze formation as would be expected considering the estimated $\Delta G°$ values for formation of H-bronzes,[17] but it was anomalously finite in others. There appeared to be no apparent correlation of the anomalous behavior with, for example, the temperature of oxidation. Anomalous behavior has been referred to elsewhere[17] when H-bronzes are formed via hydrogen spillover.

Kinetics of Hydrogen Uptake by Internally Oxidized *Pd*−Mo Alloys. The kinetics are of some interest for comparison to H-bronze formation by H spillover.[15,19] For H-bronze formation in the Pd/MoO_3 composite, the following sequential reaction steps must take place: chemisorption of H_2 on the Pd surface, chemisorbed H → absorbed H transition, H diffusion within dilute H phase of Pd, and finally, H entry and intercalation within the oxide phase. The overall rate of H-bronze formation was found to be fast, and therefore each step must be fast. Other than the step of H uptake by the internal oxide precipitates, the rates are known because they are the same as those for solution of H_2 in the dilute phase of Pd.

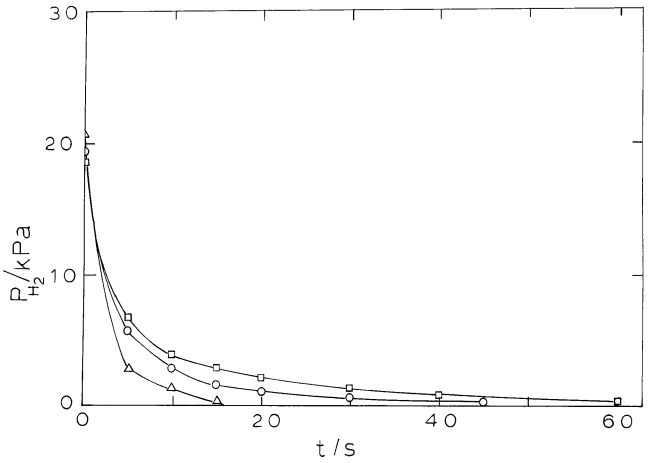

Figure 1. Plots of p_{H_2} as a function of time in the region of H-bronze formation in internally oxidized $Pd_{0.95}Mo_{0.05}$ at 323 K: (△) r = 0−0.010; (○) r = 0.010−0.0193; (□) r = 0.0193−0.0282.

These experiments are not intended to establish fundamental aspects of the kinetics of these systems but, rather, to allow some qualitative conclusions to be drawn. Figure 1 shows plots of H_2 uptake by an internally oxidized $Pd_{0.95}Mo_{0.05}$ alloy plotted as p_{H_2} against t as H reacts with the composite in a constant volume system.

In the three plots shown (Figure 1), the final $p_{H_2} \approx 0$, and thus the absorbed H is almost all in the H-bronze and not in the matrix. Over half of the H_2 is absorbed in less than 2 s for the first dose. The rates become progressively slower as r increases even though the final $p_{H_2} \approx 0$ (Figure 1). The first two steps are unlikely to be the cause of the slowing and therefore either the entrance of H into the oxide particle or H diffusion within the oxide must be the slow step. The root-mean-square (rms) distance traveled in the dilute phase of Pd is ~20 μm in 2 s (323 K) from the known H diffusion constant in the dilute phase of Pd;[20] this is comparable to the half thickness of the foil, 50 μm, and therefore diffusion within the Pd matrix is unlikely to be the slow step.

It has been reported that the diffusion constant for H within H_xMoO_3 is fast, for example, $\sim 10^{-7}$ cm^2/s at 298 K,[13] which is about the same as that in the Pd matrix.[20] Slade et al[12] also report fast diffusion but with somewhat smaller values of D_H, $\sim 10^{-8}$ cm^2/s for $H_{1.71}MoO_3$ and $\sim 10^{-11}$ cm^2/s for $H_{0.36}MoO_3$ at 300 K. The smaller D_H observed for the lower H content is contrary to the present results where the rates slow with increase of H (Figure 1). In view of the very short diffusion distances within the nanocrystalline oxides, it seems unlikely that diffusion within the oxide is the slow step. This leaves the step of H entering into the oxide as the slow one. The other steps would, of course, adjust to this slow step, for example, a pile-up of H at or near the Pd/MoO_3 interface would reduce the driving force for diffusion within the Pd matrix and its rate would then be the same as the slow step. It should be emphasized that the rate for the third and slowest determination (Figure 1) is still very fast such that about half of the H_2 is absorbed in about 3 s and, after this equilibrium is established, x (H_xMoO_3) is quite close to the maximum value found here.

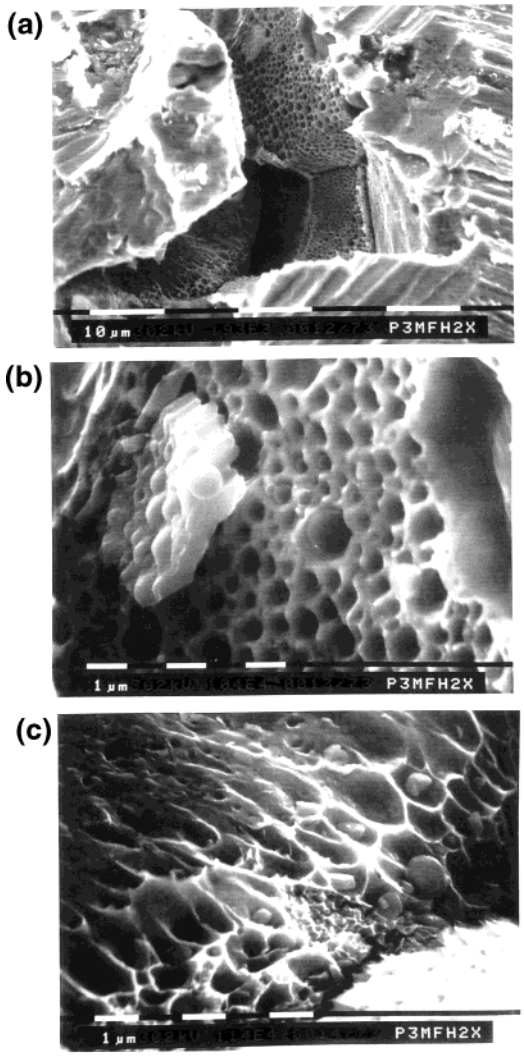

Figure 2. SEM of internally oxidized (1073 K) $Pd_{0.97}Mo_{0.03}$ alloy cycled two times: (a) photomicrograph of a cracked grain boundary resulting from cycling; (b) photomicrograph of the same cracked grain boundary as shown in panel a but at higher magnification; (c) an adjoining grain boundary.

In the conventional H-spillover technique using noble metal particles deposited on MoO_3, for example, 2% Pt, there is an induction period for the initial absorption followed by a relatively rapid intercalation process, which is complete in about 100 min at 273 K.[15] In the present work, there is no induction period. The rates of hydriding in the H-spillover studies and in the present technique can only roughly be compared. The time needed for p_{H_2} to fall to half of the initial value is about 2 s in the present work and for the reaction to be half completed in the H-spillover experiment is about 10−30 min for the second cycle and therefore the rate is about 300−900 times faster in the present technique. The greater rate found in this method of H introduction is due to the greater availability of H; for example, it is supplied to the internal oxide precipitates in all three dimensions, whereas in the spillover method the H atoms diffuse in two dimensions over the oxide surface from the metal precipitates to enter the oxide.

The slow step in H-bronze formation via H-spillover method may be one that is not a factor in the present technique, for example, transport of the H from the active Pt site over the oxide surface to a site where the H can enter the oxide.

Fripiat and Lin[21] have commented that the poor reversibility of the isotherms for H-bronzes prepared by H spillover is probably of kinetic origin, since a larger amount of H can be removed by chemical means than by simply allowing the H_2 to desorb. They state that "In H-spillover the noble metal particles (Pt for instance) are the gates by which intercalation and deintercalation proceeds", which implies that the anomalous behavior is somehow related to the H spillover. In the present method via H dissolved in the Pd matrix, none of the steps that take place on or in the Pd matrix can be irreversible. In view of this, and the fact that some irreversibility is found here, it seems that the H-spillover step from the metal to the oxide cannot be the source of the irreversibility in H spillover and therefore it must be associated with the H-bronze itself.

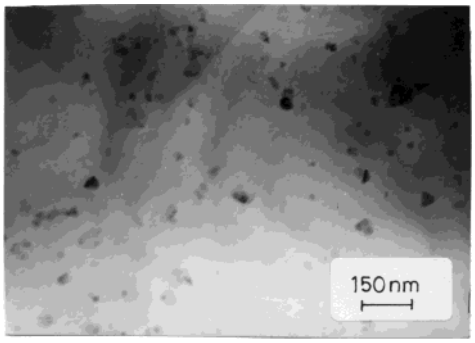

Figure 3. TEM micrograph of internal oxides formed from internal oxidation of $Pd_{0.97}Mo_{0.03}$ 1073 K showing faceted surfaces.

Scanning Electron Microscopy (SEM), Transmission Electron Microscopy (TEM), and Electron Diffraction of Internally Oxidized Alloys. SEM studies were made of the internally oxidized, cycled $Pd_{0.97}Mo_{0.03}$ alloy (Figure 2a−c). Cycling the Pd/MoO_3 composite was found to open up grain boundaries so that the grain boundaries walls can be seen with a honeycomb appearance, which was also seen in internally oxidized *Pd*−Al alloys[22] and which is caused by extrusion of Pd from the internal Pd/oxide interface as the oxide grows via vacancy transport from the surface and Pd transport away from the interface to the surface.[23] Extruded nodules of Pd can be seen (Figure 2b). The honeycomb-like grain boundary walls increase the surface area significantly and the rate of H_2 absorption.[24]

Two different internally oxidized *Pd*−Mo alloys were utilized in the TEM study, $Pd_{0.995}Mo_{0.005}$ and $Pd_{0.97}Mo_{0.03}$. TEM results for both were similar. The internal oxides, which form after internal oxidation at 1073 K for 72 h, were faceted (Figure 3) and of various sizes, for example, sizes from 4 to 30 nm in radii. Some dislocations associated with the internal oxides can be seen in Figure 4a for the internally oxidized $Pd_{0.97}Mo_{0.03}$ alloy and also for the $Pd_{0.995}Mo_{0.005}$ alloy in Figure 4b. In the latter, dislocations connect the oxide precipitates and may be pinned by them. The imaging of dislocations depends on conditions used for imaging the photograph, and this may be why they are not as apparent in Figure 3. It should be noted, however, that the dislocation density is not high indicating good accommodation of the oxide within the Pd matrix.

TEM photomicrographs were obtained for the internally oxidized $Pd_{0.995}Mo_{0.005}$ alloy *after* H-bronze formation, which was done by exposing the alloys to H_2 (323 K) at $p_{H_2} = 1.3$ kPa; this pressure is sufficient to form the Mo H-bronze but lower than that needed to form the hydride phase and therefore any dislocations introduced are not a result of hydride formation (Figure 5). After H-bronze formation, there is a greater degree of spherical contrast, which does not indicate that the precipitates become spherical but that the distortion fields around them cause the spherical contrast.

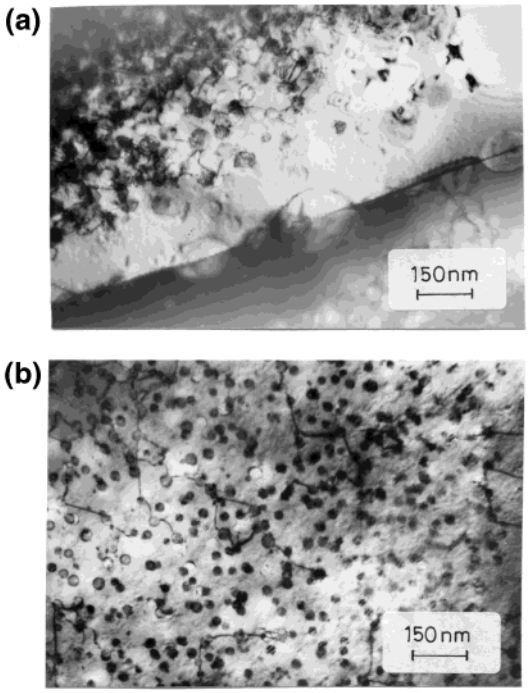

Figure 4. TEM photomicrograph of (a) internally oxidized (1073 K) $Pd_{0.97}Mo_{0.03}$ showing some dislocations and precipitates and (b) internally oxidized $Pd_{0.995}Mo_{0.005}$ alloy clearly showing dislocations connecting precipitates.

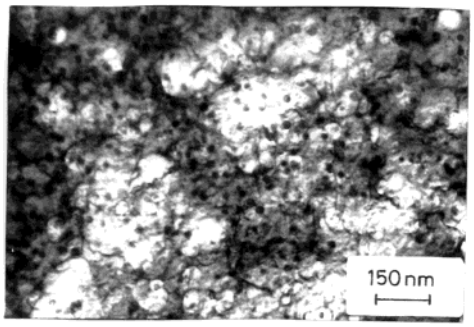

Figure 5. TEM photomicrograph of the internally oxidized $Pd_{0.995}Mo_{0.005}$ (1073 K) alloy after exposure to 1.33 kPa of H_2.

To obtain further insight about the nature of internal oxide precipitates, electron diffraction patterns were obtained. The diffraction patterns both before and after H_2 treatment were similar, and therefore the analyses are applicable to both. In Figure 6, the internal oxides are oriented with respect to the Pd matrix spots. Indexing the diffraction patterns in Figure 6a (001 zone axis) and 6b (011 zone axis) revealed that the oxide is oriented cube-on-cube with respect to the Pd matrix. The diffraction spots from the internal oxide were indexed as a cubic structure with a lattice parameter of 0.390 nm. The indexed structure can be best described by MoO_3 since the observed lattice parameter is closely related to the axes of the orthorhomic MoO_3. The lattice parameter of Pd is 0.389 nm, and therefore the MoO_3 oxides, which form within the Pd matrix, appear to accommodate themselves by forming a cubic structure.

After H_2 treatment (H-bronze formation), there is no noticeable change in the electron diffraction patterns of the oxide precipitates (Figure 7,panel a (001 zone axis) and panel b (011 zone axis)) even though the accompanying isotherms clearly indicate H-bronze formation. Therefore the H-bronze formed within the Pd matrix remains crystalline, and its lattice parameters must be very similar to those of the oxide from which

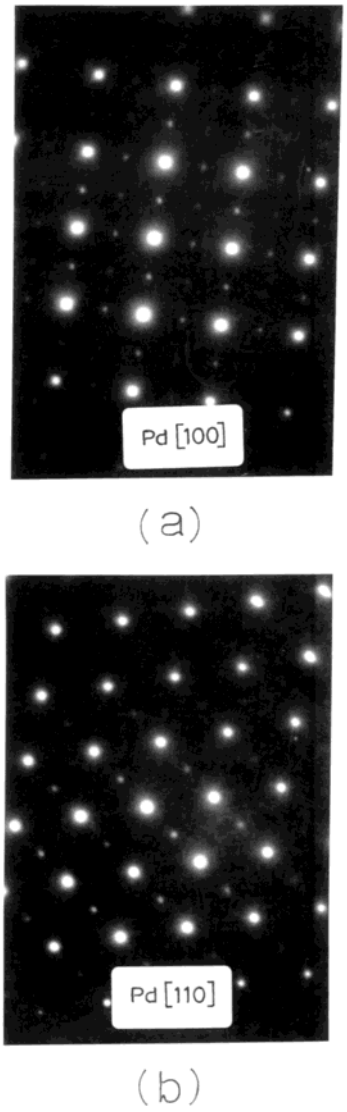

Figure 6. Electron diffraction patterns of internally oxidized (1073 K) $Pd_{0.97}Mo_{0.03}$ oriented with respect to the Pd matrix spots: (a) 001 zone axis; (b) 011 zone axis.

it is formed. The structures of H-bronzes based on molybdenum oxides are very similar to the parent oxide, and therefore electron diffraction cannot precisely determine their stoichiometry.[8] The lattice parameters of the H-bronze were based on indexing the diffraction patterns in Figure 7a,b, and the H-bronze could be any of the following: $H_{0.34}MoO_3$, $H_{0.93}MoO_3$, $H_{1.68}MoO_3$, or $MoO_2 \cdot 5(OH)_{0.5}$, but it is unlikely to be the last. The stoichiometry after exposure to H_2 at 1.33 kPa (323 K) is most likely to be closest to $H_{1.68}MoO_3$ judging from the solubility intercepts of internally oxidized $Pd_{0.97}Mo_{0.03}$ alloys (see below).

Since the lattice parameters do not change appreciably with increasing H content of H-bronzes, their stoichiometries must be determined by other means such as the strong trapping during the initial H_2 isotherm measurements. It was determined from the initial H isotherms that the H-bronze stoichiometry was $H_{1.33}MoO_3$ for the oxide formed by internal oxidation at 1093 K from the $Pd_{0.97}Mo_{0.03}$ alloy and $H_{1.67}MoO_3$ after internal oxidation at 953 K. A lower $H_{0.75}MoO_3$ stoichiometry was usually formed from internal oxidation of the $Pd_{0.98}Mo_{0.02}$ alloy. The structure of this H-bronze is monoclinic,[8] and for the reasons outlined earlier, this H-bronze appears to accommodate itself within the Pd lattice as a cubic structure with a cube-on-cube orientation with the Pd matrix.

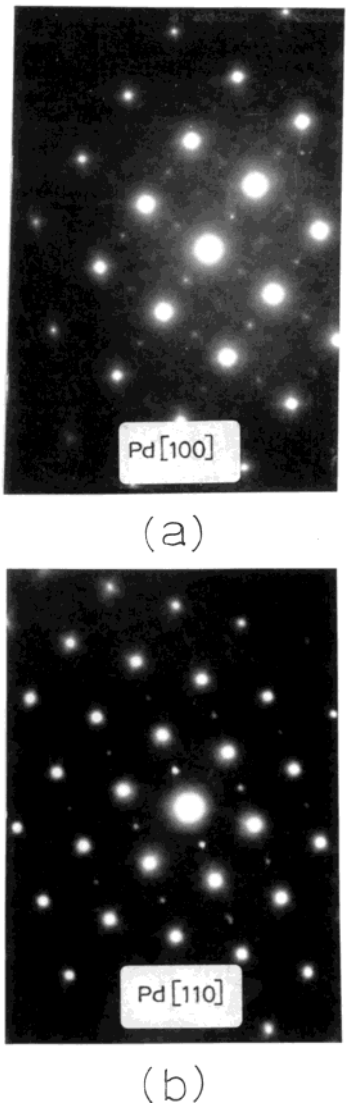

Figure 7. Electron diffraction patterns of internally oxidized (1073 K) $Pd_{0.97}Mo_{0.03}$ alloy after exposure to 1.33 kPa of H_2: (a) 001 zone axis; (b) 011 zone axis.

SANS of Internally Oxidized Alloys. Small angle neutron scattering (SANS) was carried out on the internally oxidized $Pd_{0.97}Mo_{0.03}$ and $Pd_{0.98}Mo_{0.02}$ alloys before and after exposure to H_2. The neutron scattering intensity was found to be greater for the internally oxidized $Pd_{0.97}Mo_{0.03}$ alloy than for the $Pd_{0.98}Mo_{0.02}$ alloy as might be expected. Both scattering curves indicate a distribution of oxide particle sizes. A Guinier fit of the data from $q = 0.008-0.021$ Å^{-1} gives particle radii of 7.6 and 10.6 nm for the internally oxidized $Pd_{0.98}Mo_{0.02}$ (not shown) and $Pd_{0.97}Mo_{0.03}$ alloys, respectively; this is in the general range of those observed by TEM (Figure 3) and is consistent with the expectation that larger particle sizes result from internal oxidation of alloys with larger solute contents.[25]

Figure 8 shows the scattering intensity as a function of scattering vector for the internally oxidized $Pd_{0.97}Mo_{0.03}$ alloy before and after its exposure to H to form an H-bronze; after exposure to H_2 the scattering is greater from the internally oxidized $Pd_{0.97}Mo_{0.03}$ alloy. This increase in scattering intensity (Figure 8) is due to the H within the MoO_3, which provides additional support that an H-bronze has formed because if the H were all homogeneously dissolved within the Pd matrix, the scattering intensities would be unaffected by H. According to the SANS results, the average volume of the precipitates is

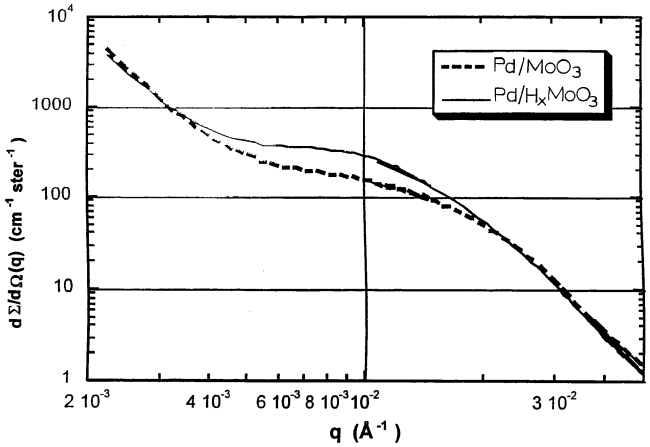

Figure 8. SANS pattern for an internally oxidized (1093 K) $Pd_{0.97}Mo_{0.03}$ alloy: (– – –) internally oxidized $Pd_{0.97}Mo_{0.03}$ alloy; (—) H containing internally oxidized $Pd_{0.97}Mo_{0.03}$ alloy.

greater after exposure to H. XRD results also indicate that there is an expansion; however, it is only about 4% when forming $H_{1.72}MoO_3$ from MoO_3.[9]

Stoichiometry of the Oxide Precipitates. The stoichiometry of the oxides formed by internal oxidation can be determined from the weight gains after oxidation. Langeler[26] found that Mo in Pd formed only poorly crystalline precipitates, but he noted, using X-ray absorption spectroscopy, that after internal oxidation at 1053 K there was a strong resemblance of the Mo K-edge to MoO_3 and none to MoO_2. For these reasons and because the electron diffraction patterns showed reflections only from MoO_3, the oxide will be referred to MoO_3 even though the weight gain after internal oxidation sometimes did not correspond very closely to it.

Five separate $Pd_{0.97}Mo_{0.03}$ alloys were internally oxidized, and most of their weight gains corresponded closely to MoO_3. After internal oxidation, the $Pd_{0.98}Mo_{0.02}$ alloys more frequently corresponded to a Mo oxide with significantly less O than MoO_3. It is not known why these different solute contents give rise to different oxides, but the result is also supported by the H trapping experiments (below) because there is less strong trapping for the internally oxidized $Pd_{0.98}Mo_{0.02}$ alloy than that expected by the 2:3 Mo ratio in these two alloys.

Hydrogen Isotherms for Internally Oxidized *Pd*-Mo Alloys. *Hydrogen Solubilities Reflecting H-Bronze (H_xMoO_3) Formation within the Pd Matrix.* It is useful to summarize the dilute phase H_2 solubility behavior in internally oxidized *Pd*–Al alloys, which do *not* form H-bronzes, for comparison with solubilities in the Pd/MoO_3 composites:[3,22] (i) there is a region of strong trapping in the very low H content region where p_{H_2} is so small that it is effectively zero at moderate temperatures for the pressure gauges employed;[3,27] (ii) after these traps are filled, H enters into the dilute phase of the Pd matrix with an enhanced solubility compared to annealed, single phase Pd, which is due to thermal residual stress in the Pd matrix surrounding the precipitate; this originates from cooling from the internal oxidation temperature and the Pd matrix and the oxide with different coefficients of thermal expansion;[27] (iii) the repeat solubility after evacuation at 323 K intersects the origin indicating that the H has not been removed from the traps; (iv) after hydriding/dehydriding and evacuation at 323 K, the solubility intercept is similar to the initial one indicating that the H trapped at or near the Pd/oxide interface has been removed.[3,22]

If a H-bronze, for example, H_xMoO_3, forms within the internally oxidized *Pd*–Mo alloys, the amount of strongly

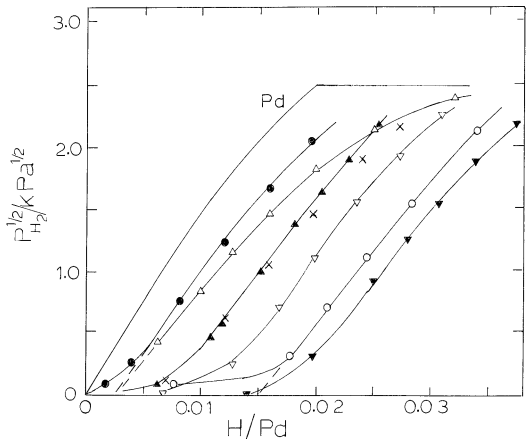

Figure 9. H_2 dilute phase solubility (323 K) in an internally oxidized (1073 K) $Pd_{0.98}Mo_{0.02}$ alloy. The symbol descriptions are given in the time sequence of the determinations: (○) initial solubility after internal oxidation; (●) repeat solubility after evacuation at 323 K (2 h); (▲) after evacuation (2 h) at 573 K; (△) after cycling through the hydride phase and evacuation (323 K); (×) after evacuation at 653 K (4 h); (▽) after evacuation at 773 K (5 h); (▼) after evacuation at 1073 K (15 h).

TABLE 1: Dilute Phase H_2 Solubility Intercepts in Pd/Mo Oxide Composites (All Completely Internally Oxidized at the Temperatures Shown)

alloy	oxidation temp (K)	initial	repeat[a]	cycled
1.5 at. % Mo	1073	0.0135	0.0017, 0.0044	
2 at. % Mo	1053	0.0110[b]	0.0018, 0.0031	
	1023	0.0155	0.0047 (12 h)	0.004 (12 h)
	1073	0.0155	0.0015 (2 h)	
	1100	0.0155	0.0025 (2 h)	0.0025
	1100	0.0160	0.0025 (12 h)	
3 at. % Mo	1100	0.0414	0.0040 (2 h)	0.0075
	1053	0.0500	0.0025 (2 h)	
	1073	0.0400		0.0025
	1073	0.0375	0.0025 (2 h)	
5 at. % Mo	1053	0.0323[b]	0.0077(12 h)	0.0064

[a] The two entries refer to 2 and 12 h evacuation, respectively. [b] The oxide lost weight during an evacuation before H_2 solubility measurements.

trapped H should be greater than that for internally oxidized *Pd*−Al alloys. This is, indeed, the case, and therefore it is clear that H-bronzes form within the Pd/oxide composites. Isotherms were measured for several different internally oxidized alloys: $Pd_{0.985}Mo_{0.015}$, $Pd_{0.98}Mo_{0.02}$, $Pd_{0.97}Mo_{0.03}$, and $Pd_{0.95}Mo_{0.05}$. Irreproducibility was sometimes encountered with H-bronze formation within the Pd/MoO_3 composites, whereas other times there was no such evidence.

Five different $Pd_{0.98}Mo_{0.02}$ alloy samples were separately internally oxidized at 1073 or 1098 K, and their subsequent H_2 solubilities were determined (323 K). Figure 9 shows dilute phase isotherms (323 K) for one of the $Pd_{0.98}Mo_{0.02}$ alloys after its complete internal oxidation (1073 K). First the "strongly trapped" H is much greater than that for Pd/oxide composites where the oxides do not form H-bronzes such as internally oxidized *Pd*−Al alloys. The five different internally oxidized $Pd_{0.98}Mo_{0.02}$ alloys, one of which was measured in a separate apparatus, had initial intercepts of $r = 0.015 \pm 0.002$ (Table 1). The value of $r = 0.015$ gives an H-bronze stoichiometry corresponding to $H_{0.75}MoO_3$. The presence of low but measurable H_2 pressures before the intercept at $r = 0.015$ differs from the internally oxidized *Pd*−Al alloys where $p_{H_2} \approx 0$ before p_{H_2} starts to increase at $r \approx 0.002$.[22]

After the initial dilute phase isotherms were measured, the composites were evacuated (323 K), and the dilute phase solubilities were remeasured. The trapping now extends to $r = 0.002$, for example, Figure 9, after a 2 h evacuation and to about 0.0035 after a 12 h evacuation. The majority of the hydrogen remains within the H-bronze after evacuation (323 K). The dilute phase solubilities can be nearly superimposed if the initial solubility curve is translated along the H/Pd axis (Figure 9) indicating there is little difference in their thermal residual stress (TRS).

There is a dilute phase solubility enhancement in the internally oxidized $Pd_{0.98}Mo_{0.02}$ alloys of $r'/r = 1.21$ (average of five samples) where r' is the H/Pd ratio for the internally oxidized alloy and r is that for Pd at the same p_{H_2} (1.2 kPa); for a $Pd_{0.97}Al_{0.03}$ alloy internally oxidized at 1073 K, $r'/r = 1.47$. The solubility enhancement may be caused by TRS, which develops during cooling of these alloys as for the internally oxidized *Pd*−Al alloys.[22]

After internal oxidation, the $Pd_{0.98}Mo_{0.02}$ alloys were completely cycled, hydrided/dehydrided, and then evacuated at 323 K; their subsequent solubilities gave an intercept of 0.003 ± 0.001. As noted above, after cycling and evacuation (323 K) Pd/oxide composites that do *not* form H-bronzes, for example, Pd/Al_2O_3 and Pd/Cr_2O_3 , *all* of their strongly trapped H is removed, whereas after evacuation alone (323 K), that is, without cycling, the trapped H is not removed.[22] This is attributed to the interaction of dislocations, which are needed to accommodate the large volume change during cycling, with the H trapped at or near the Pd/oxide interfaces. The oxide precipitates act as obstacles for dislocation movement, and thus there is expected to be a strong interaction between the moving dislocations and the precipitates and their trapped H. Cycling Pd/Mo oxide composites does not affect the majority of the trapped H, which is *within* the oxide, and consequently the intercepts are much smaller after cycling than the initial ones and similar to those for the repeat solubilities (Figure 9).

The small amount of H that is removed during cycling/evacuation may have been trapped at the interface or within the oxide. The former seems more likely because it is of the same magnitude as the H trapped at other Pd/oxide interfaces[3,22,28] and because Tinet et al[15] have stated that evacuation of $H_{1.8}MoO_3$ for 24 h at 333 K does not affect its H content.

The solubility enhancements after cycling internally oxidized $Pd_{0.98}Mo_{0.02}$ alloys are, from Figure 9, $(r'/r)_{1.2kPa} = 1.23$ (internally oxidized 1053 K) and 1.09 (internally oxidized at 1073 K) where r in the denominator is for the internally oxidized alloy. The corresponding values of $(r'/r)_{1.2kPa}$ are 1.50 and 1.26 when r in the denominator is Pd; these values are smaller than the solubility enhancement of Pd after cycling. The temperature of internal oxidation apparently is quite important for the value of the solubility enhancements. Dislocations are the main source of the solubility enhancement in cycled Pd, and they can be sufficiently annhilated by annealing at elevated temperatures ($\geq$673 K) so that the solubility enhancement is nearly eliminated; however, for internally oxidized *Pd*−Al alloys, the solubility enhancements cannot be eliminated after annealing at 823 K (48 h).[29] For internally oxidized *Pd*−Mo alloys, the solubility enhancements introduced by cycling are eliminated by lower annealing temperatures than those for the internally oxidized *Pd*−Al alloys indicating that the oxide precipitates are not such effective obstacles perhaps because of their larger size compared to the alumina precipitates.[1]

One of the internally oxidized $Pd_{0.98}Mo_{0.02}$ alloys, which had absorbed H in the dilute region to form H_xMoO_3, was evacuated

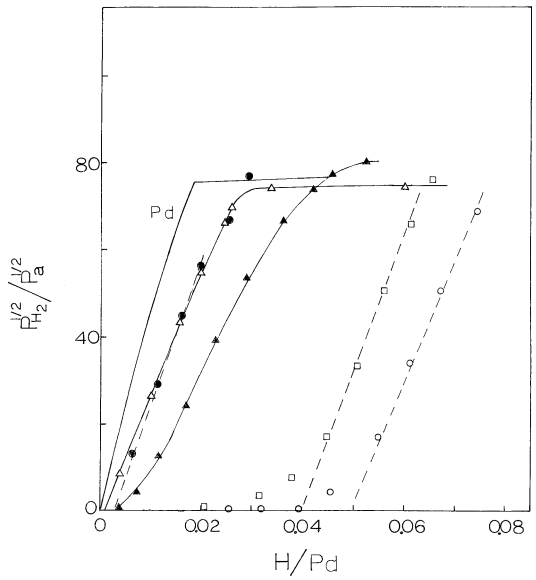

Figure 10. H_2 dilute phase solubility (323 K) in internally oxidized $Pd_{0.97}Mo_{0.03}$ alloys (1053 K). The symbol descriptions are given in the time sequence of the determinations: (○) initial solubility after internal oxidation (1053 K); (●) repeat solubility after evacuation at 323 K (2 h); (▲) after cycling through the hydride phase and evacuation; (□) initial solubility of alloy internally oxidized at 1100 K; (△) internally oxidized $Pd_{0.97}Al_{0.03}$ alloy shown for comparison.[22]

at progressively higher temperatures, and after each evacuation, H_2 solubilities were measured. Some results are shown in Figure 9 where the alloy was evacuated at the progressively higher temperatures of 573, 653, 773, and 1073 K where the latter three evacuations followed a cycling. After evacuation (2 h) at 573 K, the subsequent trapping increased to about 0.0075, but the dilute phase solubility was otherwise similar to that for the initial or repeat solubilities. The sample was then cycled, and after evacuation at 653 K (5 h), its intercept was also 0.0075, and its dilute phase solubility reflected some partial annealing of dislocations in the cycled alloy. After annealing/evacuation of this alloy at 773 K (5 h), the intercept had increased to 0.017, that is, was *greater* than the initial one. This must be due to a structural change in the oxide induced by the heating allowing it to intercalate more H. The dilute phase solubility was similar to the initial solubility indicating that the dislocation density had been reduced enough so that the solubility enhancement due to cycling had largely disappeared, but since it was still greater than that for annealed, bulk Pd, the TRS had not disappeared.

During the H_2 solubility measurements of the internally oxidized alloy following annealing at 773 K, it was observed that $p_{H_2} \approx 0$ to at least $r = 0.014$. This was observed in other experiments where, after annealing at >700 K, p_{H_2} was ~0 instead of measurable as for the initial solubility measurements following internal oxidation. After evacuation of this same internally oxidized alloy at 1073 K, its intercept decreased to $r = 0.011$. This somewhat anomalous behavior of H-bronzes has been noted by others in different situations, for example, introduction of H by spillover catalysts.[21]

Similar experiments were carried out with internally oxidized (72 h, 1073 K) $Pd_{0.97}Mo_{0.03}$ alloys, and representative dilute phase solubilities (323 K) are shown in Figure 10. The trends are similar to those found for the $Pd_{0.98}Mo_{0.02}$ alloys (Figure 9) except that the initial solubility intercepts are greater for the $Pd_{0.97}Mo_{0.03}$ alloys, that is, ~0.042 ± 0.008, corresponding to a stoichiometry of $H_{1.4}MoO_3$; this is greater than $^3/_2$($Pd_{0.98}Mo_{0.02}$ intercept) (Table 1). It is not known why this H content is greater than for that of the internally oxidized $Pd_{0.98}Mo_{0.02}$ alloys. The repeat solubility intercept for the internally oxidized $Pd_{0.97}Mo_{0.03}$ alloys is 0.003 based on results from three separate alloys after 2 h evacuations (323 K) (Table 1).

Another $Pd_{0.97}Mo_{0.03}$ alloy was internally oxidized at 1053 K, which leads to smaller precipitates; this gave an initial intercept of 0.050 corresponding to $H_{1.67}MoO_3$. It is not known why the smaller precipitates resulting from internal oxidation at a lower temperature lead to larger H contents in the H-bronze, but perhaps stress is less of a factor during subsequent H-bronze formation. The repeat solubility intercept after evacuation at 323 K was slightly smaller, $r = 0.003$ versus 0.004 for the higher temperature internal oxidation; recall that the repeat solubility for the $Pd_{0.98}Mo_{0.02}$ alloy was 0.0025 (Figure 9). After cycling, the solubility enhancement relative to the internally oxidized $Pd_{0.97}Mo_{0.03}$ alloy is 1.32 compared to 1.19 for the internally oxidized $Pd_{0.98}Mo_{0.02}$ alloy and that with respect to Pd is 1.90; this is greater than for the $Pd_{0.98}Mo_{0.02}$ alloy indicating the smaller and greater number of precipitates that form at the lower temperature interact more strongly with dislocations.

After cycling of $Pd_{0.97}Mo_{0.03}$ alloys, which were internally oxidized at 1073−1123 K, the extrapolated intercept is about 0.006 compared to about 0.003 for the $Pd_{0.98}Mo_{0.02}$ alloy. A $Pd_{0.97}Mo_{0.03}$ alloy was then evacuated at 773 K for 5 h, and its subsequent intercept was 0.023, and after evacuation at 773 K for 15 h, its intercept was 0.047. After these evacuations, the dilute phase solubilities were similar to the initial one after internal oxidation indicating that the dislocations have been annihilated sufficiently to eliminate their contribution to the solubility enhancement. The intercept after evacuation at 773 K is greater, 0.040, than the initial one following the internal oxidation, which is similar behavior to that found for the $Pd_{0.98}Mo_{0.02}$ alloy. The isotherm, $p_{H_2}^{1/2}-r$, does not extrapolate sharply to the r axis, but there is a small tail. During annealing of this internally oxidized $Pd_{0.97}Mo_{0.03}$ alloy in a closed volume (773 K), H_2 was evolved to reach values of p_{H_2} from 100 to 900 Pa, but above this temperature, the p_{H_2} spontaneously decreased to nearly zero in this closed volume. This was observed during all of the annealings at 773 K carried out for this alloy. There are obviously irreversible changes occurring within the H-bronze during the heating, for example, a rearrangement above about 500 K, which may correspond to amorphization in view of the results of Susic and Solonin.[16]

A $Pd_{0.97}Mo_{0.03}$ alloy was internally oxidized at 1073 K for 72 h, cycled, and evacuated at 653 K (5 h), after which it had an intercept of 0.018; it was then evacuated at 673 K (10 h), and its intercept was nearly the same. It was then evacuated at 873 K (1 h), and its intercept was 0.034. In the trapping region, the p_{H_2} values exhibit a nearly abrupt transition from almost zero to the dilute solubility region as compared to behavior before the higher temperature annealing treatments.

An additional $Pd_{0.97}Mo_{0.03}$ alloy was internally oxidized at 1073 K for 120 h, and its initial intercept is $r = 0.0375$ (Figure 11), and after evacuation for 2 h (323 K), $r = 0.0025$. This alloy was then evacuated for 16 h (323 K), and the remeasured solubility had an intercept of 0.004. When this alloy was then evacuated at 473 K for 3 h, the intercept was 0.014, which obviously corresponds to removal some H from within the bronze.

Stoichiometry of the H-Bronzes. The maximum content of $r = 0.0155$ for the internally oxidized $Pd_{0.98}Mo_{0.02}$ alloy corresponds to a stoichiometry of $H_{0.77}MoO_3$ assuming that all of the strongly held H enters into the oxide to form H-bronze even though a small amount <15% may be trapped at the interface.

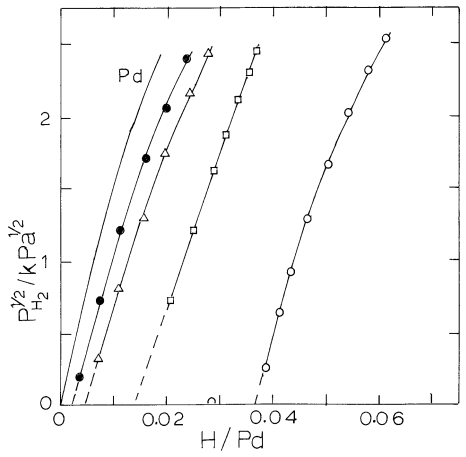

Figure 11. H_2 dilute phase solubility (323 K) in an internally oxidized (1073 K, 120 h) $Pd_{0.97}Mo_{0.03}$ alloy. The symbol descriptions are given in the time sequence of the determinations: (○) initial solubility after internal oxidation; (●) repeat solubility after evacuation at 323 K (2 h); (△) repeat solubility after evacuation at 323 K for 16 h; (□) solubility after evacuation at 473 K (3 h).

This interfacial percentage of H would decrease as the percentage of Mo in the alloy increases. The results from the initial intercepts of several internally oxidized $Pd_{0.97}Mo_{0.03}$ alloys give stoichiometries of $H_{1.40}MoO_3$ (internal oxidation at 1093 K) and $H_{1.67}MoO_3$ (internal oxidation at 953 K). Sermon and Bond[30] found a stoichiometry of $H_{1.63}MoO_3$ for an H-bronze prepared by H-spillover via 1.9% Pt. Birtell and Dickens[8] report nonstoichiometric phases extending from $x = 0.23$ to 0.4, 0.85 to 1.04, and 1.55 to 1.72. Except for internal oxidation at 1053 K, the stoichiometries found here do not correspond to any of those reported by Birtell and Dickens and may reflect the influence of stress, which develops with H-bronze formation within the Pd matrix.

The amounts of hydrogen, *x*, remaining in the H-bronze after evacuation at various elevated temperatures can be calculated by subtracting the amounts added during reabsorption (323 K) (Figure 9) from the value after the H-bronze formation, for example, $H_{1.40}MoO_3$, which was found after internal oxidation of several $Pd_{0.97}Mo_{0.03}$ alloys.

Complete Isotherms for Internally Oxidized Alloys. Figure 12 shows an isotherm for the unoxidized $Pd_{0.97}Mo_{0.03}$ alloy, which is seen to have a greater plateau pressure, a smaller H capacity, and a smaller hysteresis than Pd−H. After complete internal oxidation, this isotherm for the $Pd_{0.97}Mo_{0.03}$ alloy changes to that for Pd except for the shift in H content due to the formation of the H-bronze. The shift is also reflected in the region at the end of the plateau where p_{H_2} rises sharply with *r* in the β phase; if the *r* values at each p_{H_2} are reduced by $r \approx 0.04$, the isotherm corresponds closely to that for Pd−H. This again makes it clear that the initial traps cannot be interstices associated with the Pd lattice or else the capacity itself would be changed from pure Pd. Figure 12 also shows a repeat isotherm for an internally oxidized $Pd_{0.97}Mo_{0.03}$ alloy after evacuation at 323 K, which now corresponds closely to the Pd isotherm because there is no shift due to filling of the traps since they were already filled before the isotherm measurement. Isotherms were also measured after evacuation of this internally oxidized alloy for 5 and 12 h at 773 K. There are corresponding increased H capacities in the β-phase region after each of these treatments.

The plateau pressures for the internally oxidized $Pd_{0.97}Mo_{0.03}$ alloy are $p_f = 6.9$ kPa and $p_d = 2.7$ kPa for formation and decomposition at 323 K, respectively, as compared to $p_f = 6.2$ kPa and $p_d = 2.8$ kPa for Pd foil shown in Figure 12. Hysteresis, $^1/_2RT \ln(p_f/p_d)$, is 1.26 kJ/mol of $^1/_2H_2$ and 1.07 kJ/mol of $^1/_2H_2$ for the oxidized alloy and for Pd−H, respectively. When consideration is given to the fact that detailed isotherms and degrees of hysteresis depend on the Pd morphology, that is, spheres, foil, or small particles,[20,31,32] it is concluded that, after internal oxidation of the $Pd_{0.97}Mo_{0.03}$ alloy, the matrix is essentially Pd with regard to H_2 absorption.

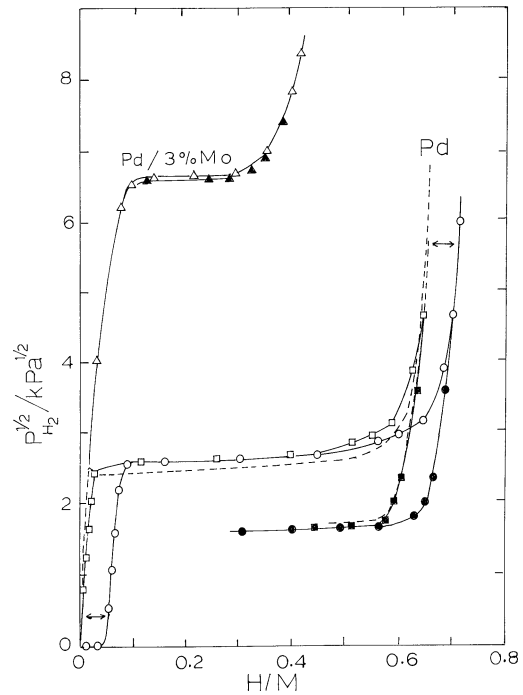

Figure 12. Complete H_2 isotherms (323 K): (△) unoxidized $Pd_{0.97}Mo_{0.03}$ alloy; (○) initial isotherm for internally oxidized (1073 K) alloy; (□) repeat isotherm after evacuation at 323 K; (− − −) annealed, single phase Pd. Open symbols denote absorption and closed ones desorption.

A $Pd_{0.97}Mo_{0.03}$ alloy that was *incompletely* internally oxidized (1073 K, 72 h) had two plateaux regions, one corresponding to Pd and the other, at a higher p_{H_2}, to the unoxidized portion of the alloy. The hysteresis for this unoxidized portion is greater than that for the unoxidized alloy. The initial isotherm shifts to higher H contents because of trapping, but the repeat isotherm does not show this because the traps are still filled after evauation at 323 K. From the relative lengths of the Pd plateau to that for pure Pd, it can be concluded that the alloy was about 70% internally oxidized. There are slightly higher plateau pressures for the Pd matrix for the repeat than for the initial cycle, but otherwise, the absorption data can be nearly superimposed when suitably shifted for trapping, showing that the H-bronze formation or the unoxidized $Pd_{0.97}Mo_{0.03}$ alloy does not affect the Pd matrix significantly with respect to H_2 absorption.

Calorimetry for the Reaction of Hydrogen with Internally Oxidized *Pd*−Mo Alloys. In most calorimetric investigations of H-bronze systems, generally one or two integral values have been obtained by reaction via H spillover, for example;[11] however, for H_xMoO_3, six integral values were determined for different *x* values by Birtill and Dickens[9] from the heats of reaction in solution of the H_xMoO_3 compounds, and these results should be independent of any irreversibility. A spectrum of decreasing $|\Delta H_H|$ values were found by Birtill and Dickens for the reacion of $^1/_2H_2$ to the oxide except possibly for a small region of nearly constant $|\Delta H_H|$ values, 60 kJ/mol of $^1/_2H_2$, in the low content region from $x = (H/MoO_3) = 0.12-0.5$.

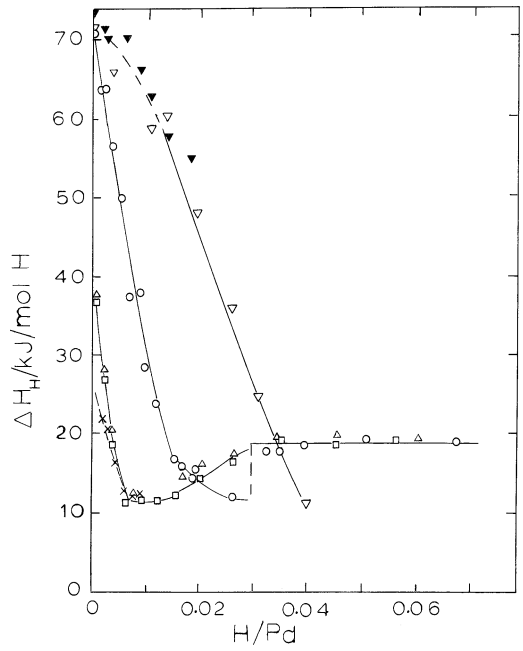

Figure 13. Calorimetric data for internally oxidized $Pd_{0.98}Mo_{0.02}$ and $Pd_{0.97}Mo_{0.03}$ alloys (303 K): (▽) initial determinations for an internally oxidized $Pd_{0.97}Mo_{0.03}$ alloy; (▼) initial determination for a different internally oxidized $Pd_{0.97}Mo_{0.03}$ alloy; (○) initial determination for a internally oxidized $Pd_{0.98}Mo_{0.02}$ alloy; (×) repeat determination for the internally oxidized $Pd_{0.98}Mo_{0.02}$ alloy after evacuation at 303 K; (△, □) determinations after cycling $Pd_{0.98}Mo_{0.02}$ alloy.

According to Birtill and Dickens,[8] four distinct phases form in H_xMoO_3 and their ranges of stoichiometry are $x = 0.23-0.4$ (orthorhombic), $x = 0.85-1.04$ (monoclinic, blue), $x = 1.55-1.72$ (monoclinic, red), and $x \approx 2.00$ (monoclinic, green) where these are approximate ranges of nonstoichometry. Therefore two phase regions would be expected from $x = 0.4-0.85$, $1.04-1.55$, and $1.72-2.00$.[9] The regions between these should be single phase where the relative partial molar properties should change continuously with x. The calorimetric results of Birtell and Dickens reflect a combination of two phase and single phase regions so that they cannot be equated to any given phase or to a two phase region. Tinet et al[11] found an integral enthalpy magnitude of 52.5 kJ/mol of $^1/_2H_2$ for the formation of $H_{1.6}MoO_3$.

Calorimetric enthalpies for H_2 absorption were measured here by adding small increments of hydrogen to the internally oxidized alloys so that the measured heats expressed per mole of H, $(\delta q/\delta n_H)$, are good approximations to the relative partial molar enthalpies, ΔH_H. In plateau regions, the heats per mole should be constant, integral values corresponding to the reaction $^1/_2H_2(g) + H_aMoO_3/(a+b) \rightarrow H_bMoO_3/(a+b)$ where a and b are the coexisting dilute and hydride phase boundaries, respectively.

The present results, like those of Birtill and Dickens,[9] show a decrease of the enthalpy magnitudes with x, and no evidence for any plateaux regions. Both the present and the earlier data of Birtill and Dickens differ from the single plateau shown in plots of p_{H_2} against r in reference;[15] however, Tinet et al noted that the plateau may not represent a true equilibrium.

Figure 13 shows some results for completely internally oxidized (1073 K for 72 h) $Pd_{0.98}Mo_{0.02}$ and $Pd_{0.97}Mo_{0.03}$ alloys. H_2 uptake by the oxide is more exothermic than the solution of H_2 in the dilute H phase of Pd where $\Delta H_H = -10.3$ kJ/mol of $^1/_2H_2$,[32] and therefore, from $r = 0$ to ~ 0.011 ($H_{0.55}MoO_3$), the amount of H in the dilute phase of Pd−H is nil. It can be concluded that absorption in this range corresponds only to H-bronze formation. When only small amounts of H are added in single phase regions the reaction is

$$\frac{1}{2}H_2(g) \rightarrow H(\text{in } H_x\text{-bronze})_{\text{at } x} \qquad (2)$$

There was no evidence of anomalous behavior in the measurements shown in Figure 13. The ΔH_H values for the internally oxidized $Pd_{0.98}Mo_{0.02}$ alloy commence at about −71 kJ/mol of H and steadily decrease in exothermicity to about −24 kJ/mol of H at $r = 0.014$ ($H_{0.70}MoO_3$) and at $r = 0.015$, $\Delta H_H = -16$ kJ/mol of H. For $r > 0.015$, the ΔH_H values continue to fall in exothermicity reaching −11.5 kJ/mol of H, which reflects mainly solution in the dilute H phase of Pd. From the corresponding p_{H_2}, the plateau pressure appears to be reached at $r = 0.035$ where the enthalpies increase in exothermicity to −18 kJ/mol of $^1/_2H_2$, which is close to the plateau enthalpy change for Pd−H.[18] The dilute/hydride phase boundary is $r = 0.018$ for Pd−H at 323 K[33] and the difference, $\Delta r = [0.035-0.018] = 0.017$, corresponds to the formation of the H-bronze, $H_{0.85}MoO_3$.

The internally oxidized $Pd_{0.98}Mo_{0.02}$ alloy was then evacuated at 323 K (12 h), and a repeat set of calorimetric measurements were carried out (Figure 13). It was found that $\Delta H_H = -22$ kJ/mol of H at $r = 0.002$, and then values fell in exothermicity to −12.0 kJ/mol of H at $r = 0.007$. Several other repeat series of calorimetric runs were carried out with evacuation at 303 K for 12 h between each series. In these, the enthalpy magnitudes were smaller than those for the first repeat set in the region between $r = 0.002$ and 0.005 but were almost the same elsewhere.

The internally oxidized $Pd_{0.98}Mo_{0.02}$ alloy was then cycled and evacuated (323 K); its subsequently measured enthalpies are more exothermic in the very dilute region than for the repeat measurements before cycling (Figure 13). The ΔH_H corresponding to the most dilute measurement is −37.5 kJ/mol of H at $r = 0.001$; the values then decrease in exothermicity becoming similar to the repeat determinations before cycling. p_{H_2} becomes measurable at $r \approx 0.003$, which corresponds to $\Delta H_H \approx -24$ kJ/mol of H. A repeat measurement of this cycled alloy gave the same $\Delta H_H - r$ behavior. It should be recalled that there is a considerable solubility enhancement after cycling Pd due to H-dislocation trapping but there is a nearly zero intercept.[32]

In Figure 14 are shown ΔH_H values for the same internally oxidized $Pd_{0.98}Mo_{0.02}$ alloy, and the corresponding p_{H_2} is measurable when $\Delta H_H \approx -24$ kJ/mol of H, which seems to be the general value when p_{H_2} commences to be measurable. The alloy was then evacuated at 473 K for 2.5 h and the calorimetric and p_{H_2} data redetermined (Figure 13). The shape of the ΔH_H against r relationship is very similar to the initial one but has been shifted to lower enthalpy magnitudes, and the intercept is smaller.

The present calorimetric results showing a sharp decrease in $|\Delta H_H|$ with r is in general agreement with the results of Birtill and Dickens.[9] There is no indication of plateaux in the present research, which might be expected from the phases found by Birtill and Dickens.[8] It is difficult to understand why $|\Delta H_H|$ decreases so markedly with r if H forms O−H and OH_2 bonds within the bronze[14] because such bonding might be expected to have similar enthalpies independent of x. On the other hand, Fripiat and co-workers[15] suggest that in view of the high mobility of H even though O−H and $O-H_2$ bonds are detected by, for example, neutron inelastic scattering,[14] the H is delocalized and such bonds have short lifetimes. This seems likely

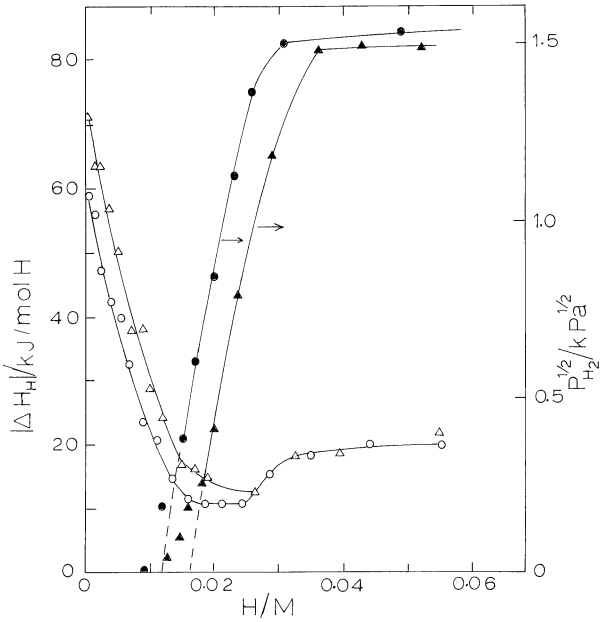

Figure 14. Data for internally oxidized $Pd_{0.98}Mo_{0.02}$ alloys (303 K): (△) initial determinations for the internally oxidized $Pd_{0.98}Mo_{0.02}$ alloy shown in Figure 13; (○) determinations for the same alloy after evacuation at 473 K. The filled symbols are the equilibrium p_{H_2} and the open symbols the corresponding calorimetric data.

as an explanation for the decrease in the $|\Delta H_H|$ values with x (Figure 13) because as noted above if there are localized O−H (O−H_2) bonds the enthalpies would be expected to be nearly constant with x.

Conclusions

When H_2 is introduced to the Pd/MoO_3 composites, it is very rapidly absorbed to form internal H-bronzes because of the availability of the mobile H atoms within the Pd matrix. H-bronzes can be formed only via H atoms. It has been shown that the amounts of hydrogen absorbed by Pd/MoO_3 composites at low p_{H_2} are much greater than the amounts absorbed by internally oxidized Pd alloys such as *Pd*−Al[3] where the latter composite traps H at the internal Pd/oxide interfaces but does not form a hydrogen bronze.

The values of x in H_xMoO_3 found here tend to be lower than those reported by other workers for macroscopic oxides and conventional H-spillover techniques or electrochemical methods to introduce H. For example, the H-bronze $x = 1.7$ was prepared by Birtill and Dickens[9] by heating the $H_{2.0}MoO_3$ compound at 383 K in a vacuum. The maximum stoichiometry found here was $H_{1.67}MoO_3$ at 303 K. The smaller amount of H may reflect the stress within the matrix and also the dimensions of the oxide precipitates, that is, nanometer. Other studies have employed "free" macroscopic oxide samples.

The $|\Delta H_H|$ values decrease markedly with x suggesting a collective effect rather than localized OH or OH_2 bond formation, that is, the H atoms must be mobile and interact with each other within the oxide.

Acknowledgment. T.B.F. acknowledges partial financial support from Westinghouse Savannah River Co. R.B. acknowledges the BOYSCAST Fellowship program from DST, India, and the University of Vermont for its hospitality while this research was carried out. The authors thank the NSF-DST for an international grant for partial support of this research. We acknowledge support of the National Institute of Science and Technology, U.S. Department of Commerce, for providing neutron facilities, and Dr. John Barker is thanked for the SANS measurements.

References and Notes

(1) Eastman, J.; Rühle, M. *Ceram. Eng. Sci. Proc*. **1989**, *10*, 1515.
(2) Huang, X.; Mader, W.; Eastman, J.; Kirchheim, R. *Scr. Met*. **1988**, *22*, 1109.
(3) Huang, X.; Mader, W.; Kirchheim, R. *Acta Metall. Mater*. **1991**, *39*, 893.
(4) Kirchheim, R.; Huang, X.; Mütschele, T. In *Hydrogen Effects on Material Behavior*; Moody, N., Thompson, A., Eds.; The Minerals, Metals and Materials Society: 1990; p 85.
(5) Noh, H.; Flanagan, T.; Balasubramaniam, R.; Eastman, J. *Scr. Mat*. **1996**, *34* 863.
(6) Flanagan, T.; Oates, W. *Annu. Rev. Mater. Sci*. **1991**, *21*, 269.
(7) Wang, D.; Noh, H.; Flanagan, T.; Balasubramaniam, R. *J. Alloys Compd*. **2002**, *348*, 119.
(8) Birtill, J.; Dickens, P. *Mater. Res. Bull*. **1978**, *13*, 311.
(9) Birtill, J.; Dickens, P. *J. Solid State Chem*. **1979**, *29*, 367.
(10) Dickens, P.; Chippindale, A.; Hibble, S.; Lancaster, P. *Mater. Res. Bull*. **1984**, *19*, 319.
(11) Tinet, D.; Partyka, S.; Rouquerol, J.; Fripiat, J. *Mater. Res. Bull*. **1982**, *17*, 561.
(12) Slade, R.; Halstead, T.; Dickens, P. *J. Solid State Chem*. **1980**, *34*, 183.
(13) Marinos, C.; Plesko, S.; Jonas, J.; Tinet, D.; Firpiat, J. *J. Chem. Phys*. **1983**, *96*, 357.
(14) Dickens, P.; Birtill, J.; Wright, C. *J. Solid State Chem*. **1979**, *28*, 185.
(15) Tinet, D.; Ancion, C.; Poncelet, G.; Fripiat, J. *J. Chim. Phys*. **1986**, *83*, 809.
(16) Susic, M.; Solonin, Y. *J. Mater. Sci*. **1989**, *24*, 3691.
(17) Fripiat, J.; Lin, X. *J. Phys. Chem*. **1992**, *96*, 1437.
(18) Flanagan, T.; Luo, W.; Clewley, J. *J. Less-Common Met*. **1991**, *172*−*174*, 42.
(19) Tinet, D.; Fripiat, J. *Rev. Chim. Miner*. **1982**, *19*, 612.
(20) Wicke, E.; Brodowsky, H. In *Hydrogen in Metals*; Alefeld, G., Völkl, J., Eds.; Springer-Verlag: Berlin, 1978; Vol. 2.
(21) Fripiat, J.; Lin, X. *Mater. Sci. Forum* **1992**, *91*−*93*, 771.
(22) Wang, D.; Noh, H.; Luo, S.; Flanagan, T.; Clewley, J.; Balasubramaniam, R. *J. Alloys Compd*. **2002**, *339*, 76.
(23) Mackert, J.; Ringle, R.; Fairhurst, C. *J. Dent. Res*. **1983**, *62*, 1229.
(24) Wang, D.; Clewley, J.; Flanagan, T.; Balasubramaniam, R.; Shanahan, K. *J. Alloys Compd*. **2000**, *298*, 261.
(25) Zhou, L.; Wei, X. *Scr. Mater*. **1999**, *40*, 365.
(26) Lengeler, B. *Ber. Bunsen-Ges. Phys. Chem*. **1986**, *90*, 649.
(27) Balasubramaniam, R.; Noh, H.; Flanagan, T.; Sakamoto, Y. *Acta Mater*. **1997**, *45*, 1725.
(28) Zhang, W.; Luo, S.; Wang, D.; Flanagan, T.; Balasubramaniam, R. *J. Alloys Compd*. **2002**, *330*−*332*, 607.
(29) Wang, D.; Balasubramaniam, R.; Flanagan, T. *Scr. Mater*. **1999**, *41*, 517.
(30) Sermon, P.; Bond, G. *Catalyis Reviews*; Marcel Dekker: 1974; Vol. 8.
(31) Kishimoto, S.; Yoshida, N.; Imamura, Y.; Hiratsuka, T.; Flanagan, T. *J. Mater. Sci. Lett*. **1993**, *12*, 1174.
(32) Luo, S.; Flanagan, T. *J. Alloys Compd*. **2002**, *330*−*332*, 29.
(33) Wicke, E.; Nernst, G. *Ber. Bunsen-Ges. Phys. Chem*. **1964**, *68*, 224.